



Solid–Liquid Equilibria of a 30 wt % Aqueous Monoethanolamine Solution Containing Urea and Monoethylene Glycol

Neerup, Randi; Kloth, Dennis S.; Almeida, Susana; Jørsboe, Jens K.; Villadsen, Sebastian N. B.; Fosbøl, Philip L.

Published in:
Journal of Chemical and Engineering Data

Link to article, DOI:
[10.1021/acs.jced.0c00758](https://doi.org/10.1021/acs.jced.0c00758)

Publication date:
2021

Document Version
Peer reviewed version

[Link back to DTU Orbit](#)

Citation (APA):
Neerup, R., Kloth, D. S., Almeida, S., Jørsboe, J. K., Villadsen, S. N. B., & Fosbøl, P. L. (2021). Solid–Liquid Equilibria of a 30 wt % Aqueous Monoethanolamine Solution Containing Urea and Monoethylene Glycol. *Journal of Chemical and Engineering Data*, 66(3), 1231–1237. <https://doi.org/10.1021/acs.jced.0c00758>

General rights

Copyright and moral rights for the publications made accessible in the public portal are retained by the authors and/or other copyright owners and it is a condition of accessing publications that users recognise and abide by the legal requirements associated with these rights.

- Users may download and print one copy of any publication from the public portal for the purpose of private study or research.
- You may not further distribute the material or use it for any profit-making activity or commercial gain
- You may freely distribute the URL identifying the publication in the public portal

If you believe that this document breaches copyright please contact us providing details, and we will remove access to the work immediately and investigate your claim.

Solid-liquid equilibria of 30 wt% aqueous monoethanolamine (MEA) solution containing urea and monoethylene glycol (MEG)

*Randi Neerup, Dennis S. Kloth, Susana Almeida, Jens K. Jørsboe, Sebastian N. B. Villadsen,
Philip L. Fosbøl**

Center for Energy Resources Engineering (CERE), Department of Chemical and Biochemical
Engineering, Technical University of Denmark (DTU), Søtofts Plads 229, 2800, Kgs. Lyngby,
Denmark

ABSTRACT:

The solid-liquid phase boundaries on new innovative solvents for the carbon capture and storage (CCS) technology have been measured in this work. The solvents have been formulated with vapour reduction additives (VRAs) also known as water lean solvents. The solid-liquid equilibrium (SLE) data will create better prediction models for the CCS technology and prevent precipitation in process equipment and thereby reduce the risk of costly shutdowns. The presented SLE data cannot be used in the prediction of solid formation in condenser as it would require knowledge of the vapour-liquid-solid equilibria.

The SLE of the systems urea-H₂O, urea-monoethanolamine (MEA)-H₂O, and monoethylene glycol (MEG)-H₂O have been determined using the methods freezing point depression (FPD) and SLE by FPD. 61 new SLE data points are listed of $0 < w(\text{urea}) < 60 \%$, and $0 < w(\text{MEG}) < 20 \%$.

It is the first time that the ternary systems have been measured. The eutectic temperatures were found at $-8 \text{ }^\circ\text{C}$ for urea-H₂O and $-27 \text{ }^\circ\text{C}$ for urea-MEA-H₂O. Highly concentrated urea solutions freeze completely upon mixing water with MEA due to the endothermic reaction. Solubility data of MEG-MEA-H₂O was found for $t > -40 \text{ }^\circ\text{C}$. All SLE points for MEG in 30 wt% aqueous MEA freezes below $-15 \text{ }^\circ\text{C}$.

To avoid clogging from urea precipitation, it is recommended to use urea below 30 wt%.

1. Introduction

Global warming is partially caused by the dependency on fossil fuels. Therefore, alternative energy sources such as biogas are researched as alternative fuels. Biogas is currently a largely unexploited energy resource produced from biological sources such as waste water and residual biomass. Typically biogas contains 25-50 % CO₂, 50-75 % methane and impurities such as water, hydrogen sulfides, ammonia and volatile organic components (VOC)^{1,2}.

The presence of CO₂ in the biogas leads to a low calorific value of around 8 kWh/m³ which can be increased to 15 kWh/m³ by removing CO₂³. This process is called first-generation biogas upgrading⁴. The upgraded biogas can be injected into the gas grid to replace natural gas from fossil fuel.

The first-generation upgrading process removes the CO₂ in an absorption process utilizing chemical solvents such as aqueous amines. The technology is also known as acid gas removal. In this process, CO₂ is removed from biogas or another gas which enters the absorber column from the bottom at 40 °C counter-current with the lean solvent that is fed in on the top of the column. The rich solvent, containing absorbed CO₂, leaving the bottom of the absorber is heated in a cross heat exchanger with the lean solvent coming from the stripper column. The solvent is boiled in the bottom of the stripper. The desorber is usually operated at 100-120 °C. The rich solvent enters the stripper and CO₂ is released at the top. The hot lean solvent from the stripper is cooled in the cross heat exchanger and recycled to the absorber. The separated CO₂ can be stored in geological formations, and/or be used for downstream products in food, feed, and pharmaceutical industries or for welding applications.

The upgrading process is energy intensive, and research into energy reducing methods is ongoing. One such method is applying vapour reduction additives (VRAs, also known as water lean solvents) to reduce the vaporization of the solvent in the desorption process and thereby effectively lowering the energy requirements. The addition of VRA to MEA reduces the amine vapour pressure causing more water vapour pressure reduction, resulting in less reboiler duty. The VRA technology and the water lean CO₂ capture solvents are new developments and a limited amount of information is available for these solvent systems,⁵⁻⁸. While these sources focus on reduced amine vaporization, they observe 10-25% reduced energy consumption. Most likely this is caused by less water vaporization. While the additives reduce the amine vapour pressure, they reduce the water vapour pressure more. The VRAs could have unforeseen adverse effect on fluid properties and it still remains to be proved if the VRA gives an overall improvements of the CO₂ capture concept.

MEA is as a benchmark solvent known for fast reaction with CO₂. The disadvantage of using MEA is the high energy demand for the desorption process. The high energy consumption can be reduced by VRAs. The aim of adding VRA to a solvent like MEA is to increase the boiling point of water and thereby reduce vaporisation.

The aim of this study is to investigate the solid-liquid equilibrium phase boundary of MEA solvent formulations containing VRA. The VRAs investigated in this study are urea and monoethylene glycol (MEG). The effect on adding VRA to 30 wt% monoethanolamine (MEA) is investigated for the purpose of characterizing solvent behaviour with temperature, and of thermodynamic modelling of CO₂ capture. The extended UNIQUAC thermodynamic model can be applied to systems including VRA for the purpose of optimizing CO₂ capture systems. The SLE of respectively urea and MEG in aqueous solutions of MEA have previously not been examined.

Urea and monoethylene glycol (MEG) are studied as potential VRAs. Urea has been used worldwide as nitrogen-releasing agent in agricultural fertilizer^{9,10}. Furthermore it has been used as a reducing agent to lower the NO_x emissions from diesel engines^{11,12}. MEG has mainly been used in antifreeze formulations¹³ and as raw material in the polyester fibre fabrication^{14,15}. Additionally, MEG has also been known to prevent hydrate formation in wet gas transport pipelines and gas processing plants^{16,17}.

Table 1 shows the solid phase boundaries of urea-H₂O, and MEG-H₂O studied by several authors. Concentration and temperature range are presented in Table 1 and graphically presented in Figure 1 and Figure 2.

To conclude on the SLE data, Table 1 only few have measured the freezing curve of urea in water. Freezing points of urea in water were measured by Hausrath¹⁸ and Chadwell and Politi¹⁹.

Several authors^{20, 21, 22, 23-24} have studied the solubility in the concentration range 40-76 wt% urea. Solubility up to 132 °C was measured by Berliner²⁵ and Miller and Dittmar²⁶.

The literature data on the MEG-H₂O system is limited to four authors. This is surprising since the system has been used for decades on many industrial processes. The solubility of MEG in water in the whole concentration range was studied by Ross²⁷, Cordray et al.²⁸, and Ott et al.²⁹. The phase diagram of MEG in water reveals two eutectic points near -49 °C and -43 °C, and a hydrate with the local maximum at ≈ 77.5 wt% MEG. Ott et al.²⁹ and Ross²⁷ reported also the forming of metastable phases.

SLE of the ternary systems MEA-urea-H₂O, and MEA-MEG-H₂O have not been considered in the literature.

Table 1. Literature review on SLE data for the systems: urea-H₂O, and MEG-H₂O.

Author	Year	Component	Concentration (wt%)	Temperature (°C)
Hausrath ¹⁸	1902	Urea	0.01 to 0.25	0 to -0.08
Pinck and Kelly ²¹	1925	Urea	40 to 76	0 to 70
Shnidman and Sunier ²²	1932	Urea	51 to 76	18 to 70
Miller and Dittmar ²⁶	1933	Urea	75 to 100	68 to 132
Berliner ²⁵	1936	Urea	40 to 96	0 to 120
Chadwell and Politi ¹⁹	1938	Urea	2 to 33	-0.6 to -11.5
Bergman and Sulaimankulov ²³	1959	Urea	57.5	30
Druzhinin et al. ³⁰	1967	Urea	57	30
Druzhinin and Kondratieva ³¹	1967	Urea	54	25
Kondrat'eva and Druzhinin ³²	1968	Urea	54	25
Pavlenko ³³	1971	Urea	54	25
Lee and Lahti ²⁰	1972	Urea	41 to 72	1.8 to 60
Tembotov and Druzhinin ²⁴	1973	Urea	57	30
Ross ²⁷	1954	MEG	0 to 95	0 to -53
Ott et al. ²⁹	1971	MEG	0 to 100	0 to -49
Cordray et al. ²⁸	1996	MEG	0 to 100	0 to -49
Baudot and Odagescu ³⁴	2004	MEG	40 to 50	-22 to -36

2. Experimental details

2.1 Materials

The chemicals: MEA, MEG, and urea used in this study are shown in Table 2. They were used as received without further purification. The sample mixtures were prepared with deionised water with a conductivity of 0.2 $\mu\text{S}/\text{cm}$. When preparing the mixtures water was substituted with VRA. The MEA concentration was 30 wt% in all mixtures.

Table 2. Chemicals used in the experiments.

Chemical name	Source	CAS No.	Mass fraction purity	Purification method
Monoethanolamine	Sigma-Aldrich	141-43-5	≥ 0.99	none
Urea	Sigma-Aldrich	57-13-6	≥ 0.99	none
Monoethylene glycol	Sigma-Aldrich	107-21-1	0.998	none

2.2 Apparatus

Freezing points were measured using a modified Beckmann apparatus. Temperature was controlled by a thermostatic cooling/heating bath (Julaba MR, Julaba FP50). Sample temperature was recorded by an Agilent 34970A data acquisition unit connected to a PC. The temperature probe was a Pt100 DIN 1/10 made with a handle. The sample glass is fitted with a magnetic stirrer and a lid. The lid of the sample glass is connected to a rubber stopper. The temperature probe and a platinum wire stirrer surrounds the temperature probe are penetrated through rubber stopper and lid. The platinum wire stirrer can be moved up and down. The same setup is used for solubility measurements at temperature above 0 °C. A full description of the setup has been described in detail by Fosbøl et al.^{35,36}.

2.3 Experimental method

The detection of a freezing point firstly includes the addition of a sample mixture into a sample glass. The sample glass is cooled by placing it in an ethanol bath, which is controlled by a thermostatic bath. The temperature of the thermostatic bath is kept 5 °C below the expected freezing point of the sample mixture. As a freezing point is located the sample glass is removed from the ethanol bath and heated in the air until micro ice crystals are left in the sample solution. This procedure is repeated five times.

The solubility of VRA in 30 wt% MEA at temperatures above 0 °C is determined by visually inspecting the melting of the solid precipitates of either urea or MEG. The same setup used for freezing point determinations is used to cool the sample solution until precipitation. When precipitation is observed, the sample is taken out of the ethanol bath and heated. The disappearance of the last crystal is recorded by the Pt 100 temperature probe which is used in the FPD setup.

Manual stirring in the form of a stainless steel wire stirrer, which is moved up and down, is applied in both methods in order to maintain a uniform sample temperature. Each sample solutions have been replicated five times to obtain reproducible results. Standard deviations up to ± 0.2 °C are observed using the FPD and the SLE by FPD methods. Before measurements, the Pt100 temperature probe is calibrated against known freezing point values of aqueous NaCl solutions. The experimental work were conducted at atmospheric conditions.

A detailed description of the freezing point depression (FPD) method is described elsewhere by Fosbøl et al.³⁶. This method is applicable for detection of ice. Details of the method, named SLE by FPD, for measuring solubility above 0 °C is outlined elsewhere by Fosbøl et al.³⁵.

3. Results and discussion

3.1 The urea-H₂O and MEA-urea-H₂O systems

The experimental solubility results of urea in water and urea in mixtures of MEA-H₂O are presented in Table 3 and Table 4 together with literature data¹⁴⁻²⁵ on urea-H₂O. The SLE temperatures, standard deviations, and information on solid formation are all listed in the tables.

$w(\text{urea})$ is the concentration of urea on MEA free basis. All experiments were conducted at atmospheric pressure. Figure 1 shows the SLE phase boundaries of the systems: urea-H₂O, and urea-MEA-H₂O.

Standard deviations up to ± 0.2 °C were obtained in some cases. The reproducibility is decreasing when using the SLE by FPD method. This is expected as the melting of precipitates is visually inspected³⁵.

In the urea-H₂O system the eutectic point, E_1 , is at the temperature -11 °C, see Figure 1. Ice is formed at $w(\text{urea}) < 0.33$. Above the eutectic temperature urea is precipitating.

The eutectic temperature, E_2 , of the system of urea-MEA-H₂O is approximately located at -27 °C. Ice starts forming at -15 °C until the eutectic point and at $w(\text{urea}) > 0.21$ solid urea precipitates. No indication of hydrate formation was observed in the urea-H₂O, and urea-MEA-H₂O systems. MEA tend to have little impact on the urea solubility in water. The solubility curve for both systems show quite normal expected trends for ice formation as a parabolic decreasing curve is observed until the eutectic point. Above the eutectic point, where urea precipitates, the curve trend is convex in nature. It is expected that the SLE curve to increase with a concave tendency. The behaviour is related to the enthalpy, heat capacity, and activity of the dissolved urea. The curve indicates that

these parameters will have quite unusual or non-ideal magnitudes. A significant endothermic heat of dissolution was observed, while mixing urea into water.

The experimental SLE data obtained in this work is in line with the literature¹⁴⁻²⁵ on urea-H₂O. Minor outliers are revealed in the study by Pinck and Kelly²¹ at $w(\text{urea}) = 0.67$ and $w(\text{urea}) = 0.72$, which creates valuable information in the context of the accuracy of thermodynamic modelling.

The addition of MEA decreases the solubility of urea in water and in the mixture of 30 wt% MEA as seen in Figure 1. The eutectic point moves to the left from $w(\text{urea}) = 0.33$ in pure water to $w(\text{urea}) = 0.21$ in 30 wt% MEA. The temperature is also much lower than for urea in water. As urea starts precipitating, the two solubility curves are following the identical linear trend.

At atmospheric conditions, solid urea decomposes around 130 °C to biuret and later to cyanuric acid³⁷⁻⁴⁰. Normal CO₂ capture with MEA is operated at 120 °C. Use of VRA could cause a boiling point elevation of 5 °C. To lower the boiling point, preventing e.g. urea decomposition, the stripper could be run 0.1 bar lower than normal operation pressure of 1.8 bar. A decrease of 0.1 bar reduces the boiling point temperature corresponding to VRA addition. As the use of VRA may change the pressure in the stripper and impact the need for compression and the performance of the overall capture plant. The solubility data above 130 °C obtained by Miller and Dittmar²⁶ might be biased by decomposition products.

The use of urea as VRA in solvent formulation for CCS may create challenges often observed when dissolving chemicals. Mixing the solvent with concentrated urea creates an endothermic reaction, which at $w(\text{urea}) = 0.30$ makes the solvent freeze completely. It can be recommended to heat the solvent while dissolving urea. Addition of urea to the solvent may reduce the stripper pressure in order to avoid solvent degradation. This could offset savings in the reboiler duty.

Urea will like any other salt precipitate at high concentration. The solid phase diagram of urea in water and in 30 wt% MEA can be used to prevent solid formation in the plant. Formulation of 30 wt% MEA with urea should under normal conditions be below $w(\text{urea})= 0.30$. Operational condition during wintertime at Artic and Scandinavian condition could entail other minimum design specifications.

Table 3. SLE temperatures of the binary urea-H₂O system. The SLE temperatures are given at Pressure $p = 0.1$ MPa^a

Urea	t	u_t^b	Solid phase
g/g total	°C	°C	
0	0.00	0.0	Ice
0.025	-0.68	0.029	Ice
0.050	-1.41	0.04	Ice
0.075	-2.28	0.017	Ice
0.100	-2.82	0.059	Ice
0.125	-3.60	0.032	Ice
0.150	-4.35	0.057	Ice
0.175	-5.27	0.024	Ice
0.200	-6.17	0.042	Ice
0.225	-7.00	0.046	Ice
0.250	-8.01	0.042	Ice
0.275	-8.98	0.051	Ice
0.300	-10.03	0.043	Ice
0.310	-10.26	0.044	Ice
0.315	-10.59	0.028	Ice
0.320	-10.76	0.051	Ice
0.325	-10.98	0.052	Eutectic composition
0.330	-10.06	0.054	Urea
0.335	-8.90	0.144	Urea
0.340	-7.98	0.112	Urea
0.350	-6.47	0.114	Urea
0.375	-2.96	0.052	Urea
0.400	0.93	0.185	Urea
0.425	4.86	0.193	Urea
0.450	8.58	0.152	Urea
0.475	12.70	0.082	Urea
0.500	16.76	0.064	Urea
0.550	25.55	0.032	Urea
0.600	35.14	0.1	Urea

^aStandard uncertainties (u) for the temperature, weight fractions, and the pressure are $u_c(t) = \sqrt{u^2(\text{calibration}) + u^2(\text{repeatability})} = 0.05$ °C, $u(w) = 0.001$, $u(p) = 1$ kPa. Temperatures are reported as the standard deviation of the mean in the table. ^bStandard deviations of five consecutive analysis.

Table 4. Solubility data of the ternary MEA-urea-H₂O system. The SLE temperatures are given at Pressure $p = 0.1 \text{ MPa}^a$.

MEA	Urea	Urea	t	u_t^b	Solid phase
g/g total	g/g total	g/g (water + urea)	°C	°C	
0.300	0	0	-14.92	0.050	Ice
0.300	0.025	0.036	-17.07	0.055	Ice
0.300	0.050	0.071	-18.48	0.017	Ice
0.300	0.075	0.107	-20.65	0.023	Ice
0.300	0.100	0.143	-22.49	0.029	Ice
0.300	0.125	0.179	-24.75	0.059	Ice
0.300	0.130	0.186	-25.32	0.064	Ice
0.300	0.135	0.193	-25.52	0.072	Ice
0.300	0.140	0.200	-26.14	0.077	Ice
0.300	0.145	0.207	-26.86	0.083	Ice
0.300	0.150	0.214	-27.24	0.050	Eutectic composition
0.300	0.155	0.221	-24.73	0.094	Urea
0.300	0.160	0.228	-23.14	0.017	Urea
0.300	0.165	0.236	-21.84	0.063	Urea
0.300	0.170	0.243	-20.44	0.14	Urea
0.300	0.175	0.250	-19.24	0.04	Urea
0.300	0.200	0.286	-13.57	0.10	Urea
0.300	0.225	0.321	-8.03	0.080	Urea
0.300	0.250	0.357	-2.71	0.10	Urea
0.300	0.275	0.393	2.40	0.044	Urea
0.300	0.300	0.429	7.54	0.062	Urea
0.300	0.325	0.464	12.93	0.044	Urea
0.300	0.350	0.500	18.97	0.031	Urea

^aStandard uncertainties (u) for the temperature, weight fractions, and the pressure are $u_c(t) = \sqrt{u^2(\text{calibration}) + u^2(\text{repeatability})} = 0.05 \text{ °C}$, $u(w) = 0.001$, $u(p) = 1 \text{ kPa}$. The temperatures are also reported as the standard deviation of the mean in the table. ^bStandard deviations of five consecutive analysis. The concentration of urea is presented twice. The concentration in terms of g/g total reflects the real solubility in the multicomponent mixture. The concentration is also presented in terms of MEA free basis g/g(water + urea) which greatly improves the comparison basis in the figures.

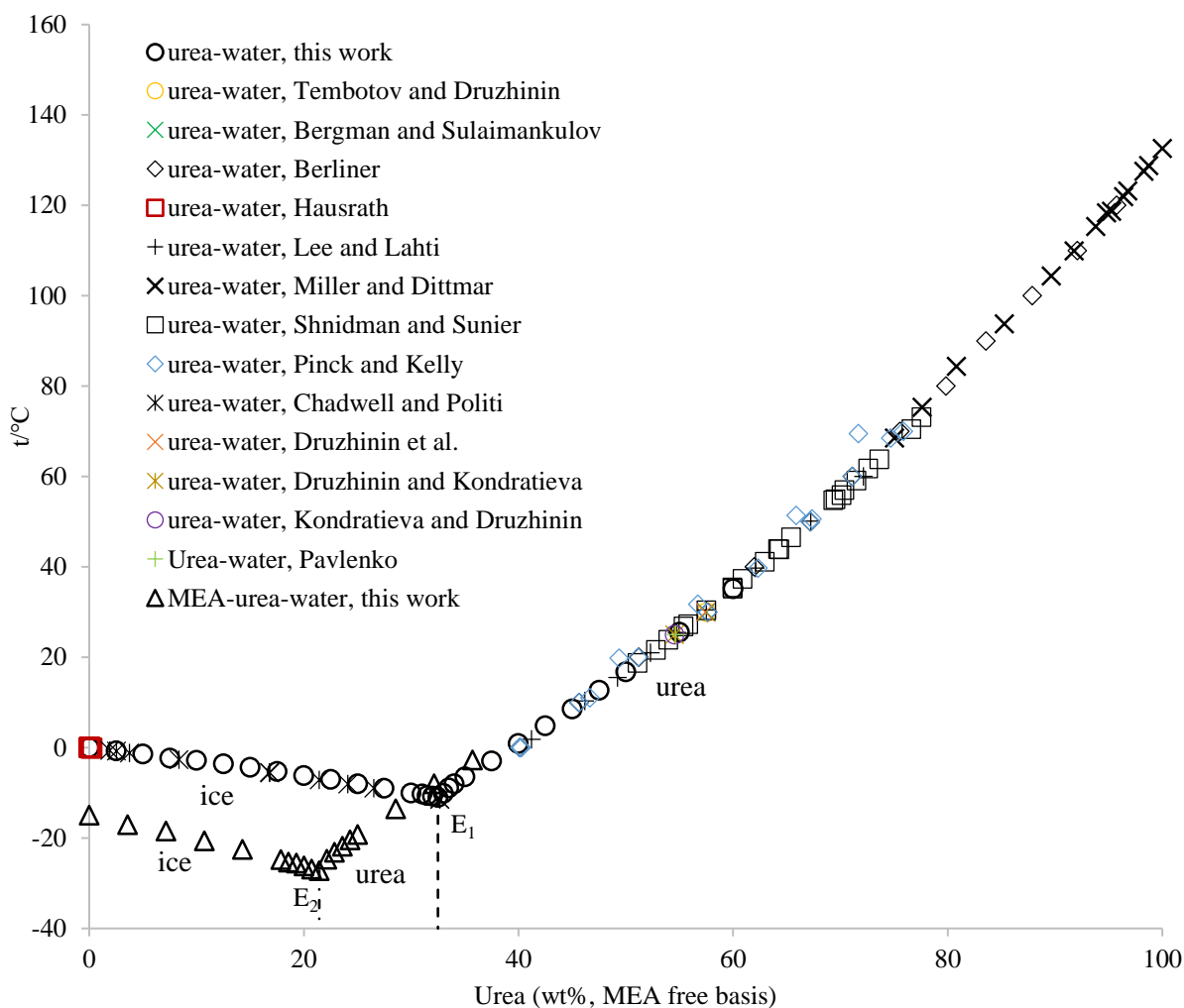


Figure 1. SLE diagram of solid precipitation in urea-H₂O, and in urea-MEA-H₂O as a function of temperature at atmospheric conditions. Vertical lines represents the eutectic composition. E: eutectic temperature. The SLE data for urea-H₂O are taken from the literature¹⁸⁻²⁹.

3.2 The MEG-MEA-H₂O system

The measured solubility data for MEG in 30 wt% MEA are graphically presented in Figure 2. The corresponding SLE data are given in Table 5 together with standard deviations and

information on solid precipitation. A repeatability better than 0.1 °C was obtained indicating a good accuracy. The FPD method was used for all experimental data points in the MEG-MEA-H₂O system. $w(\text{MEG})$ is the concentration on MEA free basis.

Figure 2 shows the SLE curve for MEG-MEA-H₂O and the literature data²⁶⁻²⁹ for MEG-H₂O. The freezing curves for both systems illustrate expected behaviour with parabolic trend. The MEA does not change the parabolic behaviour to a large extent. The SLE diagram for MEG-MEA-H₂O only presents concentrations of $w(\text{MEG}) \leq 0.20$ and $t > -40$ °C. The sample mixtures above this concentration were too viscous when cooling down and due to limitation of the cooling bath, it was not possible to obtain solid precipitates. Ice was formed in the analysed concentration range and there was no indication of hydrate formation.

The SLE phase diagram of MEG-H₂O, shows two eutectic points at -49 °C and at -43 °C and the existence of a hydrate with the local minimum at approximately $w(\text{MEG}) \approx 0.75$. The two data points, indicated with red circles in Figure 2, at -53 °C and -52 °C was reported as metastable points by Ross²⁷. Comparing the two phase diagrams the freezing points of MEG-MEA-H₂O is decreased with $\Delta t \approx 15$ °C.

Based on the SLE diagram of MEG-MEA-H₂O there is no risk of solid formation or clogging in a CCS plant during wintertime as the solid formation occurs below -15 °C.

There is a need for a more detailed study of the solid phase boundary of MEG-MEA-H₂O for $w(\text{MEG}) > 0.20$ even though it may not be relevant in a CCS perspective it will be important for the precision of thermodynamic modelling.

Table 5. SLE data of the ternary MEG-MEA-H₂O system. The SLE temperatures are given at Pressure $p = 0.1$ MPa^a.

MEA	MEG	MEG	t	u_i^b	Solid phase
g/g total	g/g total	g/g (water + MEG)	°C	°C	
0.299	0	0.000	-14.92	0.050	Ice
0.300	0.025	0.036	-17.21	0.073	Ice
0.300	0.050	0.071	-19.48	0.068	Ice
0.300	0.075	0.107	-21.93	0.064	Ice
0.300	0.100	0.143	-24.33	0.025	Ice
0.300	0.125	0.179	-27.47	0.082	Ice
0.300	0.150	0.214	-30.12	0.090	Ice
0.300	0.175	0.250	-34.35	0.031	Ice
0.300	0.200	0.286	-37.75	0.060	Ice

^aStandard uncertainties (u) for the temperature, weight fractions, and the pressure are $u_c(t) = \sqrt{u^2(\text{calibration}) + u^2(\text{repeatability})} = 0.05$ °C, $u(w) = 0.001$, $u(p) = 1$ kPa. The temperatures are also reported as the standard deviation of the mean in the table. ^bStandard deviations of five consecutive analysis. The concentration of urea is presented twice. The concentration in terms of g/g total reflects the real solubility in the multicomponent mixture. The concentration is also presented in terms of MEA free basis g/g(water + urea) which greatly improves the comparison basis in the figures.

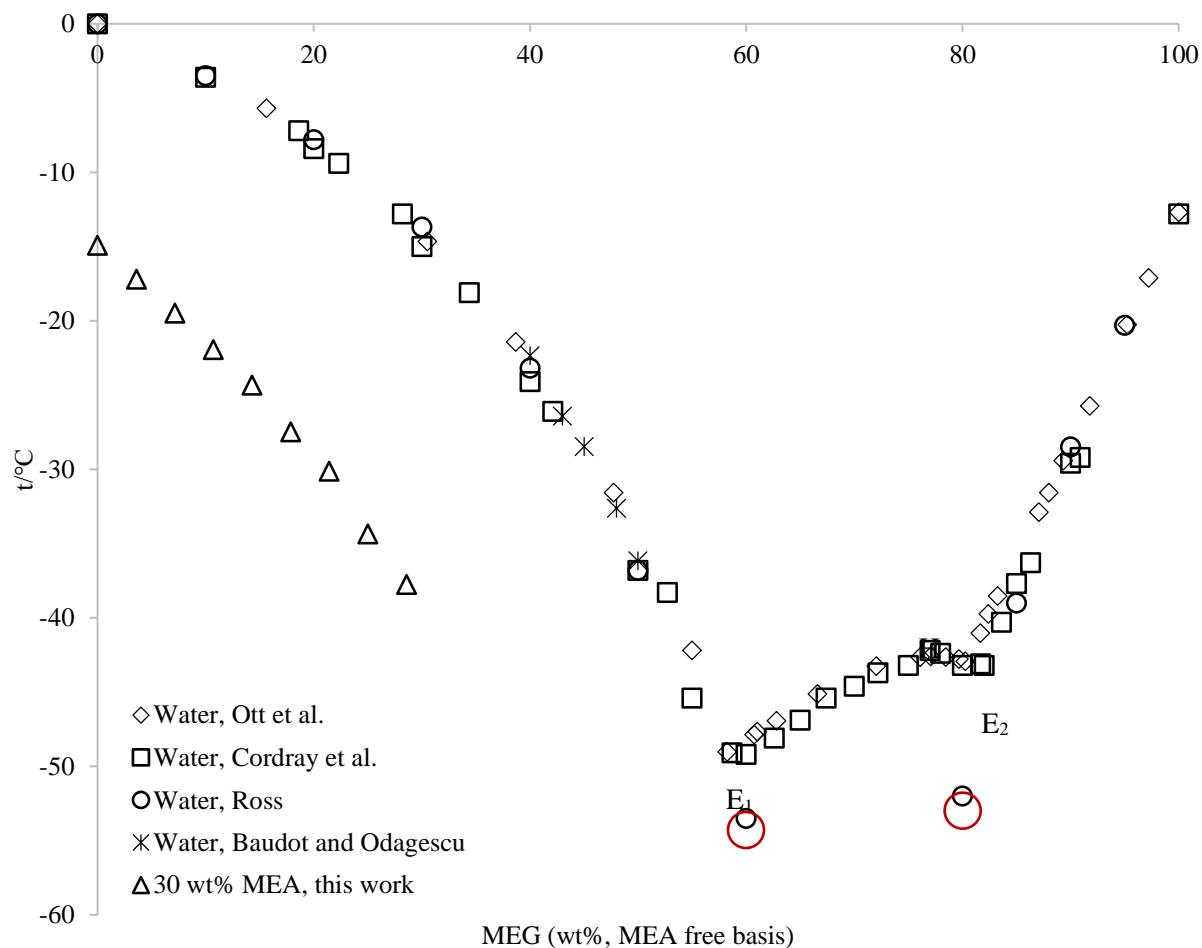


Figure 2. Solid phase boundary of MEG-MEA-H₂O and of MEG-H₂O as a function of temperature. Solubility data of MEG-H₂O is obtained from the literature³¹⁻³⁴. E: eutectic point, H: hydrate. The red circles indicate the metastable points reported by Ross²⁷.

4. Conclusion

In this work, the solubility of the binary system urea-H₂O and the ternary systems urea-MEA-H₂O and MEG-MEA-H₂O were determined using the two experimental methods freezing point depression (FPD) and solid-liquid equilibria (SLE) by FPD. In total 61 new data points were determined in the temperature range spanning from -40 to 35 °C.

The SLE data for urea-H₂O was compared to the literature and it agreed well. For the urea-MEA-H₂O system ice is forming until the eutectic temperature of -27 °C. Above the eutectic temperature urea is precipitating. No hydrates were observed in the urea-MEA-H₂O system. For liquid precipitation, urea can be used as a VRA in 30 wt% MEA up to a concentration of ≈30 wt%. At higher concentrations, solids will form and this will create clogging in a CCS plant. The SLE diagram of MEG in 30 wt% aqueous MEA indicated that ice is forming below -15 °C. Due to cooling limit of the cooling bath, the eutectic temperature was not revealed.

Solid formation in condenser etc. cannot be predicted based on the above results. Such an evaluation would require knowledge of the vapour-liquid-solid equilibria, not studied here. On the other hand, data from this work can contribute to the formation of a thermodynamic calculation basis, which enables evaluations of condenser or similar other types of unintended precipitation phenomena.

There could be solvent challenges which are not clear currently but need to be investigated in the future. These could be the influence of lowering the stripper pressure on the reboiler duty savings, corrosion, mass transfer restrictions, and reaction limitations in terms of kinetics.

The presented SLE data will contribute to quality of thermodynamic modelling of new innovative CO₂ solvents for the CCS technology.

AUTHOR INFORMATION

Corresponding Author

*E-mail: plf@kt.dtu.dk. Tel.: + 45 4525 2868.

Contributions

The manuscript was written through contributions of all authors. All authors have given approval to the final version of the manuscript.

Funding Sources

The funding from the BioCO₂ project (the Danish government through the EUDP agency no 64016-0082) and the financial support from the Center for Energy Resources Engineering (CERE), and the Technical University of Denmark.

ABBREVIATIONS

CCS, carbon capture and storage; DSC, differential scanning calorimetry; FPD, freezing point depression; MEA, monoethanolamine; MEG, monoethyleneglycol; SLE, solid-liquid equilibrium; VRA, vapour reducing additives

REFERENCES

- (1) Wellinger, A.; Murphy, J. D.; Baxter, D. *The Biogas Handbook. Science, production and applications 2013*, Woodhead Publishing Series in Energy, number 52.
- (2) Ryckebosch, E.; Drouillon, M.; Vervaeren, H. *Techniques for transformation of biogas to biomethane. Biomass and Bioenergy 2011*, 35, 1633-1645.
- (3) International Organization for Standardization, ISO 6976:2, *Natural gas - Calculation of calorific values, density, relative density and Wobbe indices from composition*, 2016.
- (4) Villadsen, S. N. B.; Fosbøl, P. L.; Angelidaki, I.; Woodley, J. M.; Nielsen, L. P.; Møller, P. *The Potential of Biogas; the Solution to Energy Storage. ChemSusChem. 2019*, 12, 2147-2153.
- (5) Heldebrant, D. J.; Koech, P. K.; Glezakou, V.; Rousseau, R.; Malhotra, D.; Cantu, D. C. *Water-Lean Solvents for Post-Combustion CO₂ Capture: Fundamentals, Uncertainties, Opportunities, and Outlook. Chem. Rev. 2017*, 117, 9594-9624.
- (6) Conway, W.; Beyad, Y.; Feron, P.; Richner, G.; Puxty, G. *CO₂ absorption into aqueous amine blends containing benzylamine (BZA), monoethanolamine (MEA), and sterically hindered / tertiary amines. Energy Procedia. 2014*, 63, 1835-1841.
- (7) Conway, W.; Beyad, Y.; Richner, G.; Puxty, G.; Feron, P. *Rapid CO₂ absorption into aqueous benzylamine (BZA) solutions and its formulations with monoethanolamine (MEA), and 2-amino-2-methyl-1-propanol (AMP) as components for post combustion capture processes. Chem Eng J. 2015*, 264, 954-961.
- (8) Puxty, G.; Conway, W.; Botma, H.; Feron, P.; Maher, D.; Wardhaugh, L. *A New CO₂ Absorbent Developed from Addressing Benzylamine Vapour Pressure Using Co-solvents. Energy Procedia. 2017*, 114, 1956-1965.

- (9) Bremner, J. M.; Krogmeier, M. J. Elimination of the adverse effects of urea fertilizer on seed germination, seedling growth, and early plant growth in soil. *Proc Natl Acad Sci U S A*. 1988, 85, 4601-4604.
- (10) Mikkelsen, R. L. Biuret in urea fertilizer. *Fertil Res*. 1990, 26, 311-318.
- (11) Koebel, M.; Elsener, M.; Kleemann, M. Urea-SCR: a promising technique to reduce NOx emissions from automotive diesel engines. *Catal Today*. 2000, 59, 335-345.
- (12) Guan, B.; Zhan, R.; Lin, H.; Huang, Z. Review of state of the art technologies of selective catalytic reduction of NOx from diesel engine exhaust. *Appl Therm Eng*. 2014, 66, 395-414.
- (13) Rosen, J. S.; Szkutak, M. D.; Jaskolka, S. M.; Connolly, M. S.; Notarianni, K. A. Engineering performance of water mist fire protection systems with antifreeze. *J Fire Prot Eng*. 2013, 23, 190-225.
- (14) Świergiel, J.; Jadzyn, J. From supramolecular to conventional polymers: Polyethylene glycol. *Phys Chem Chem Phys*. 2018, 20, 6045-6049.
- (15) Ma, H.; Hyun, J.; Stiller, P.; Chilkoti, A. "Non-Fouling" Oligo(ethylene glycol)-Functionalized Polymer Brushes Synthesized by Surface-Initiated Atom Transfer Radical Polymerization. *Adv Mater*. 2004, 16, 338-341.
- (16) AlHarooni, K.; Barifcani, A.; Pack, D.; Gubner, R.; Ghodkay, V. Inhibition effects of thermally degraded MEG on hydrate formation for gas systems. *J Pet Sci Eng*. 2015, 135, 608-617.
- (17) Seo, Y.; Kang, S. P. Inhibition of methane hydrate re-formation in offshore pipelines with a kinetic hydrate inhibitor. *J Pet Sci Eng*. 2012, 88-89, 61-66.
- (18) Lee, F. M.; Lahti, L. E. Solubility of Urea in Water-Alcohol Mixtures. *J Chem Eng Data*. 1972, 17, 304-306.

- (19) Pinck, L. A.; Kelly, M. A. The Solubility of Urea in Water. *J Am Chem Soc.* 1925, 47, 2170-2172.
- (20) Shnidman, L.; Sunier, A. A. The solubility of urea in water. *J Phys Chem.* 1932, 36, 1232-1240.
- (21) Berliner, J. F. T. Crystal urea. *Ind Eng Chem.* 1936, 28, 517-522.
- (22) Miller, F. W.; Dittmar, H. R. The Solubility of Urea in Water. The Heat of Fusion of Urea. *J Am Chem Soc.* 1934, 56, 848-849.
- (23) Bergman, A. G.; Sulaimankulov, K. Equilibria in the systems: water-urea-cobalt sulphate and water-urea-copper sulphate. *Russ J Inorg Chem.* 1959, 4, 420-423.
- (24) Druzhinin, I. G.; Murzubraimov, B.; Rysmendiev, K. The $\text{NiCl}_2\text{-CO}(\text{NH}_2)_2\text{-H}_2\text{O}$ system at 30°C. *Russ J Inorg Chem.* 1967, 12, 1037-1038.
- (25) Druzhinin, I. G.; Kondratieva, N. G. The solubility diagram of the system cobalt sulfate-cobalt nitrate-urea-water. *Khim Khim Tekhnol.* 1967, 10, 1187-1190.
- (26) Kondrat'eva, N. G.; Druzhinin, I. G. Solubility in the ternary systems of Cobalt nitrate or sulfate in aqueous urea solutions at 25°C. *Uch Zap Mosk Obl Pedagog Inst.* 1968, 193, 151-161.
- (27) Pavlenko, A. I. The systems $\text{MnCl}_2\text{-urea-H}_2\text{O}$ and $\text{CoCl}_2\text{-urea-H}_2\text{O}$ at 25°C. *Ukr Khim Zh.* 1971, 37, 415-418.
- (28) Tembotov, B. K.; Druzhinin, I. G. Nickel sulphate-urea-water system at 30°C. *Russ J Inorg Chem.* 1973, 18, 1372-1373.
- (29) Hausrath, H. Eine differentialmethode zur bestimmung kleiner gefrierpunktsdepressionen. *Zeitsehr f Phys Ohern.* 1902, 37, 522-554.
- (30) Chadwell, H. M.; Politi, F. W. The Freezing Points of Concentrated Aqueous Solutions of Urea, Urethan, and Acetamide. *J Am Chem Soc.* 1938, 60, 1291-1293.

- (31) Ross, H. K. Cryoscopic Studies - Concentrated Solutions of Hydroxy Compounds. *Ind Eng Chem*. 1954, 46, 601-610.
- (32) Cordray, D. R.; Kaplan, L. R.; Woyciesjes, P. M.; Kozak, T. F. Solid - liquid phase diagram for ethylene glycol + water. *Fluid Phase Equilib*. 1996, 117, 146-152.
- (33) Ott, J. B.; Goates, J. R.; Lamb, J. D. Solid-liquid phase equilibria in water + ethylene glycol. *J Chem Thermodyn*. 1972, 4, 123-126.
- (34) Baudot, A.; Odagescu, V. Thermal properties of ethylene glycol aqueous solutions. *Cryobiology*. 2004, 48, 283-294.
- (35) Fosbøl, P. L.; Neerup, R.; Arshad, M. W.; Tecle, Z.; Thomsen, K. Aqueous solubility of piperazine and 2-amino-2-methyl-1-propanol plus their mixtures using an improved freezing-point depression method. *J Chem Eng Data*. 2011, 56, 5088-5093.
- (36) Fosbøl, P. L.; Pedersen, M. G.; Thomsen, K. Freezing Point Depressions of Aqueous MEA, MDEA, and MEA–MDEA Measured with a New Apparatus. *J Chem Eng Data*. 2011, 56, 995-1000.
- (37) Jones, J. M.; Rollinson, A. N. Thermogravimetric evolved gas analysis of urea and urea solutions with nickel alumina catalyst. *Thermochim Acta*. 2013, 565, 39-45.
- (38) Zhang, H.; Xi, Y.; Su, C.; Liu, Z. G. Lab Study of Urea Deposit Formation and Chemical Transformation Process of Diesel Aftertreatment System. *SAE Tech Pap*. 2017,
- (39) Shahariar, G. M. H.; Lim, O. T. A study on urea-water solution spray-wall impingement process and solid deposit formation in urea-scr de-nox system. *Energies*. 2019, 12, 1-18.
- (40) Tischer, S.; Börnhorst, M.; Amsler, J.; Schoch, G.; Deutschmann, O. Thermodynamics and reaction mechanism of urea decomposition. *Phys Chem Chem Phys*. 2019, 21, 16785-16797.

For Table of Contents Only

